

RESEARCH ARTICLE

Implementing B-Spline Path Planning Method Based on Roundabout Geometry Elements

HANG CAO  **AND MATE ZOLDY**

Department of Automotive Technologies, Budapest University of Technology and Economics, 1111 Budapest, Hungary

Corresponding author: Hang Cao (hang.cao@edu.bme.hu)

This work was carried out at the Budapest University of Technology and Economics supported by the National Research Development and Innovation Fund, TKP2020 National Challenges Subprogram based on the charter of bolster issued by the National Research Development and Innovation Office through the auspices of the Ministry for Innovation and Technology under Grant No. BME-NC.


ABSTRACT This paper presents a parametric B-spline-based path planning approach for roundabout exit traverse planners to handle successively generated trajectories. A roundabout is a complex driving scene because of its large curvature and the varying intersection leg angles. A few studies focus on the relationship between roundabout intersection leg angle and path performance. This paper discusses B-spline advantages to curve road conditions and the impact of roundabout geometry elements on path planning performance. Knot vectors are defined, and control points are calculated to meet the requirements for generating paths that fit in different roundabout direction maneuvers. Four countries' roundabout design standards are summarized with their unique geometry elements. Additionally, the Stanley tracking controller was used to calculate the steering behavior. The impacts of maneuver directions and intersection angles are discussed. It is explained stepwise how the maneuver system framework was built and what notable impacts the geometric structure of the roundabout has on the paths.

INDEX TERMS Roundabout, geometry elements, path planning, B-spline.

I. INTRODUCTION

Over the decades, there have been many breakthroughs in autonomous vehicle (AV) mobility and safety work. This noteworthy progress of self-driving vehicles is well-developed; however, many achievements still need to be accomplished by governments and industries to exploit intelligent systems dealing with different driving scenarios [1]. Advanced driver assistance systems can now better manage some traffic scenario cases than human behavior [2]. Because of the limited sensor range and map accuracy, navigation in a driving environment can be a challenge for autonomous vehicles [3].

Path planning is essential for navigation processes among all navigational tasks. Because all AVs need to move from the starting point to the destination no matter what the mission is. Path planning technique has been discussed since the 1970s [4]: global and local path planning have been addressed, depending on the environment and the information of obstacles. Path planning techniques are differentiated based upon the environment type, i.e. well-known environment and partially-known environment.

The associate editor coordinating the review of this manuscript and approving it for publication was Razi Iqbal .

Developing intelligent path planning algorithms is one of the most critical issues when designing maneuver architectures under different road conditions. Roundabouts are a challenging scenario in urban environments. Although automated planning on the highway scenario is maturing, the roundabout scenario condition has been argued thoroughly since 2013. Roundabouts still represent an unsolved challenge for developing a robust autonomous system among all the test scenes. Gonzalez *et al.* summarized the path generation methods, listed the motion planning techniques in automated driving scenarios [5], and applied a proper parametric-based path planner based on a French roundabout type [6]. The authors generated the path to each exit with a Bézier curve. Chen *et al.* conducted lane change path with a piecewise Bézier curve in the XY plane, planning the vehicle trajectory on the ego path and the speed profile according to the cubic Bézier approach. The ego car velocity is calculated by dividing the setting function in the Z axis [6]. Driving behaviors in roundabouts were introduced in [7] and [8], and an Model Predictive Control (MPC) planner fitting in mini-roundabout conditions was built in [9].

This paper aims to solve the path planning and path tracking problem related to road geometry elements, i.e., considering roundabout design aspects at single-lane roundabouts.

The proposed framework is based on the parametric B-spline method, and the path is generated via predefined waypoints. Knot vectors and control polygons show the feature of path shape, fitting in different country standards. The simulation experiment results lead in two directions that simulate different path movements as maneuver directions. Then entry angle, entry radius, exit radius, and circle diameter are considered as variables to illustrate the relationship between intersection angle and path performance.

The main contributions of this study are proposed as:

- Generate path according to roundabout road condition, use uniform B-spline interpolating the first and last point of the path, govern the continuity and smoothness of connection points.
- Integration of road structure data features for single-lane roundabouts in different countries, route constraints and waypoints selection can be carried out uniformly and efficiently.
- Test the relationship between the roundabout intersection angle and path performance.

The rest structure of the paper is as follows. Section 2 reviews the advantages of the spline-based path planning method and path following technique in the Stanley control strategy. Section 3 introduces the basic function of the B-spline method; relevant mathematical functions will also be illustrated there. The problem and solution for system planner architecture will be presented in Section 4. Section 5 represents the system planning method and the tracking controller strategy. The discussion on driving behavioral planning and results are presented in Section 6. Finally, Section 7 delivers the concluding remarks.

A. RELATED WORK

1) PATH PLANNING IN B-SPLINES

Recently, path planning techniques mainly include four methods [10]: graph-search-based, sampling-based, interpolating curve-based, and numerical optimization. Graph Search Based Planners solve the path problem by visit vary space grids. For example, Dijkstra Algorithm is used to find the single-source shortest path in the graph [11] and A* algorithm solves the problem via searching the fast node. Sampling-based planner mainly includes RRT algorithm, some researchers applied the RRT solution in the roundabout scenario [12], [13], provided a fast and random search through navigation space, and have been used to solve the path planning problem. However, less consideration was given to distinguishing structural differences between different sections of the roundabout road condition, such as the path constraints that the exit radius is larger than the radius of the entry area. Using the interpolation method can avoid this kind of road structure definition error. The interpolation method solves the problem with road waypoints selection, which is determined by the road structure and boundary constraints. The advantage of the global interpolation planning method is that it can be used in the case of a lack of scene information from onboard sensors and communication network systems.

To present the curve path, implicit, explicit, and parametric expressions are allowed. The most common methods for the interpolation curve method are B-spline, Bézier, and rational Bézier curves [14]. Compared to Bézier curves, B-splines are more complex, and the main difference between them is the complexity of their mathematical definition. Bézier curves allow fast computation and fast manipulation [14]. Han *et al.* present the right-turn Bézier curve in the intersection and illustrates the use of k -th order initial path and cut path to find the shortest curve path. Some research presents anti-collision work with the 4th-order of Bézier curve, meeting the computation and manipulation requirements [15].

For parametric curves, two main problems can be addressed. Firstly, the autonomous vehicle's initial trajectory definitions vary; secondly, the proposed path should fit the obstacle in real-time to adapt to the dynamic environment.

B-spline curves were developed to overcome the limitations of Bézier curves: the need for local control of the curve, the difficulty in imposing C2 continuity, and the fact that control points of a Bézier curve determine its degree [16].

The B-spline algorithm uses segmented continuous multi-segment generation and consists of piece by piece curves. Gloderer *et al.* used Akerman's vehicle motion model to create spline paths. A set of waypoints was given, minimizing the transverse time to create an appropriate trajectory. The authors also presented scenario cases to validate the algorithm and showed the optimization results [17]. Connors *et al.* set the path planner using the basis splines technique (B-spline) via limited control point sets to reach the pre-defined maneuver [18].

Meanwhile, Berglund *et al.* present eight cases validating that the geometrically designed paths are smooth and fast to traverse. The paper considered fourth-degree, uniform B-spline methods to smooth the path and implement obstacle avoidance proposals [19]. Additionally, Ahmed *et al.* proposed a framework using the Genetic Algorithm (GA) to ensure path smoothness requirements. Both segmented polynomial and B-spline approaches have been used in the main contributions to reach the optimization goal of path length and safety. They use path potential field approach to adjust the environment complexity. To eliminate the collision probability, the researchers minimize the sum of obstacles and maximize the entire path spotting area [20]. Kano *et al.* planned spline trajectories satisfying the smooth requirements and giving an upper overcome bound on the curvature [21]. Mercy *et al.* exploited spline properties to minimize nonlinear optimization results and guarantee constraint satisfaction [22]. Maekawa *et al.*'s algorithm can deal with opposite direction path data and reach collision avoidance [23]. The authors obtain the vehicle's obstacle information, states, headings, and the transverse area's boundary. They accomplish path planning through cubic B-spline curve to interpolate the initial and end positions data. However, there will be slight slope curvature discontinuity at path knots. Ghilardelli *et al.* proposed a parameterized curve method for heavy trucks, introducing η^4 splines by

calculating eight parameters to define the path condition or change the path direction. A parking case path generation was illustrated as well [24].

The B-spline method maintains the Bézier curve advantages and overcomes the disadvantage of lack of local properties because of the integral representation. Moreover, B-spline solves the connection problem when running complex shapes.

B. PATH FOLLOWING ADVANTAGES IN STANLEY CONTROL

The most common techniques for AVs path following are Pure Pursuit method, Stanley method, and MPC tracking model. These techniques play an essential role in the autonomous navigation field and apply to different environments and road conditions. Ji *et al.* focused on the sliding corner case [25]. Daoud *et al.* applied both lane and double-lane change maneuvers to execute the numerical solution for the path following problems [26]. Liu *et al.* fixed the path following issue considering circular bends under four different quadrants [27].

Researchers focus on integrated path planning and path tracking methods as well. Model predictive method is used more frequently in integrated path planning and tracking tasks because of their numerical optimization characteristic. The constraints are manually set as a range in most of the work. Li *et al.* supposed a novel integrated framework based kinematically-feasible path to deal with spatial path planning problems. The actuators' dynamics constraints are implemented by restricted steering angle range. The model uncertainty took part in combined feedforward and feedback lateral control strategy [28]. Huang *et al.* used nonlinear Model Predictive algorithm to optimize the dynamic constraints, i.e., the front wheel angle and brake torque, to reach the single lane change maneuver [29]. Cao *et al.* proposed a Model predictive function to optimize roundabout road constraints and vehicle stability [30]. Constraints have flexible and multiple ways to handle in the integrated framework. Receding horizon optimization (RHO) was used to solve the wheel torque and steering input constraints [31]. Ellenrieder *et al.* proposed a speed and path-following controller that solved the dynamics constraints with equivalent control. The control input was combined and mixed in the model, introduced human cognition with a novel storage function, and used super-twisting second-order sliding mode to implement human-machine shared control on the path following [32]. These methods concentrate more on vehicle ego constraints, with few mentions of the scenario road constraints.

Both Pure Pursuit controller and Stanley controller belong to the geometric path tracking method. Geometric methods are less impressionable to path smoothness, the shortage of waypoints, and positioning errors [33]. Unlike Pure Pursuit measures the distance from the rear axis, the Stanley controller uses the central point of the front axis. Furthermore, the Stanley controller features a correction for yaw difference and a corresponding correction for the path tracking by cross-track error.

The Pure Pursuit method needs a careful choice of the look-ahead distance [34] among geometric path-following methods. However, the Stanley control can avoid the disadvantage and allow instant vehicle speed. Dominguez *et al.* maintain good tracking precision at a low speed [35]. Abdelmoniem *et al.* used a modified Stanley controller to test six different maneuver roads, such as hook road, S curve road, curve Highway road, lane change road, multiple lane change road, and straight road [34].

In most of the above work, the proposed solutions handle path planning and path tracking issues with specific curve roads or continuous curvature roads. The planner in this paper deals with path curves at different angles within the range of the roundabout standards[36] permits, including large curvature roads and non-continuous curves.

II. FUNDAMENTAL THEORY OF B-SPLINE CURVE

This section introduces the essential functions of the B-spline curve related to the topic.

A. NONUNIFORM B-SPLINES

The de-Boor-cox recursive algorithm is the most popular method for deriving the B-spline basis functions [37], [38]. The non-uniform B-splines (NURBS) function's zero-degree general expression provides good model shaping, which is accurate and flexible [39]–[45].

$$B_{j,0}(t) = \begin{cases} 1, & t_{j+1} \leq t \leq t_{j+1}, j \geq 1 \\ 0, & \text{otherwise} \end{cases} \quad (1)$$

Building with non-decreasing order knots vectors, NURBS express the piecewise basis of splines as follows,

$$B_{j,n}(t) = \left(\frac{t - t_j}{t_{j+n} - t_j} \right) B_{j,n-1}(t) + \left(\frac{t_{j+n+1} - t}{t_{j+n+1} - t_{j+1}} \right) \times B_{j+1,n-1}(t) \quad (2)$$

After a linear combination of basis functions and weighting factors, the control points or de Boer points are obtained and calculated as,

$$f(t) = \sum_0^{m-n-2} P_1 B_{1,n}(t), t \in (t_n, t_{m-n-1}) \quad (3)$$

B. UNIFORM B-splines

Uniform B-spline function consists of uniformly and equidistantly distributed knots along the parameter axes. A characteristic of a uniform B-spline is its equal distance between two nearby knots. The integrated expression of uniform B-splines is

$$B_{j,n}(t) = \frac{n}{n+1} \sum_{i=0}^{n+1} \omega_{i,n}(t - t_i)_+^n (t - t_j) = 0, \dots, m-n-1 \quad (4)$$

where

$$\omega_{i,n}(t) = \prod_{j=0, j \neq i}^{n+1} \frac{1}{t_j - t_i}$$

For a uniform B-spline curve, the matrix expression of its equation takes the form

$$C_i(t) = [1 \ t \ \dots \ t^k] M_k \begin{bmatrix} d_{i-k} \\ d_{i-k+1} \\ \vdots \\ d_i \end{bmatrix} \quad (5)$$

where the coefficients are $M_k(k = 1, 2, 3)$ are

$$M_1 = \begin{bmatrix} 1 & 0 \\ 0 & 1 \end{bmatrix}, M_2 = \begin{bmatrix} 1 & 1 & 0 \\ -2 & 2 & 0 \\ 1 & -2 & 1 \end{bmatrix},$$

$$M_3 = \begin{bmatrix} 1 & 4 & 1 & 0 \\ -3 & 0 & 3 & 0 \\ 3 & -6 & 3 & 0 \\ -1 & 3 & -3 & 1 \end{bmatrix}$$

Their expression in matrix form is

$$f(t) = \frac{1}{6} [P_0, P_1, P_2, P_3] \begin{bmatrix} 1 & 4 & 1 & 0 \\ -3 & 0 & 3 & 0 \\ 3 & -6 & 3 & 0 \\ -1 & 3 & -3 & 1 \end{bmatrix} \begin{bmatrix} t^3 \\ t^2 \\ t \\ 1 \end{bmatrix} \quad (6)$$

To match the first and last points of the curve to the first and latest data points, respectively, we need to make sure the first and last points $p+1$ conditions and their calculations, i.e.,

$$0 = u_0 = u_1 = \dots = u_p \leq u_{p+1} \leq \dots \leq u_{m-p}$$

$$= u_{m-p+1} = u_m = 1$$

$$u_0 = u_1 = \dots = u_p$$

$$\begin{cases} u_j = u_{j-1} + \frac{1}{m-2p} (j = p+1, \dots, m-p+1) \\ u_{m-p} = u_{m-p+1} = \dots = u_m \end{cases} \quad (7)$$

III. PROBLEM STATEMENT

Travelling through the roundabout requires the vehicle to generate path smoothly, considering geometrical elements and fitting in the realistic road condition. A roundabout has its characteristics because of the unique road geometry. Several particular parameters distinct from the highway can affect the driving behavior, such as the number of entrances and exits, path calibration, traffic rules, geometric frame setting, or lane number [27]. As for the geometric-based path planning and control point generation, we propose that the roundabout driving condition identify three stages, i.e., entrance, circulatory roadway, and exit, as Figure 1 shows.

The entry angle, shown in Figure 2, is the angle of conflict between entering traffic and circulating traffic. In general, too low an entry angle produces poor viewing angles in the turning direction, causing drivers to look over their shoulders, which is complex, and may encourage merging behavior similar to freeway ramps. At the same time, too high an entrance angle may not provide sufficient positive alignment to deter staggered traffic, reduce capacity, and may produce excessive entrance excursions that can lead to sharp braking at the entrance with rear-end collisions [36]. Therefore, national traffic road design standards are an essential indicator for

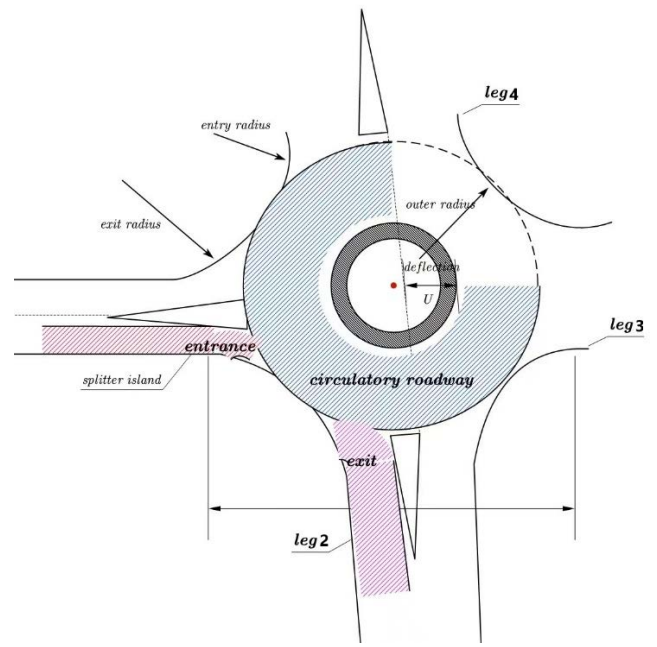


FIGURE 1. Driving condition stages in roundabouts.

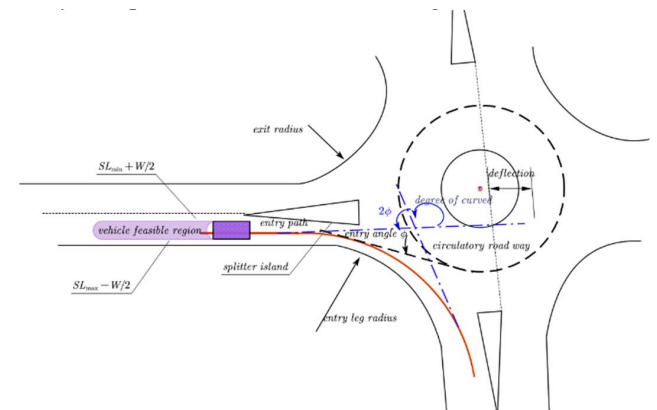


FIGURE 2. Roundabout geometry elements and vehicle path constraint.

planning vehicle behavior. The needs of road conditions make vehicle behavior vary from country to country. The exit radius is slightly larger than the entrance radius, allowing vehicles to exit the roundabout more smoothly, except for the different entrance angles.

A roundabout setting is used to reduce the traffic junction, and the primary purpose is to let the vehicle go through the intersection safely. In this case, the primary goal for path planning is to let the vehicle transverse the roundabout comfortably and smoothly. Algorithm 1 shows the main phases of vehicle driving behavior when passing through the roundabout. This setting differs from other road conditions, and it is crucial to check vehicle driving conditions in circulating roads when approaching the roundabout merging zone. When the ego car finds itself in the safety phase, the global planner starts to plan the maneuver based on the exit going decision.

Due to the actual vehicle structure and the road geometry characteristics, the system needs to satisfy the following constraints as the data in Table 1. We summarize the geometric

Algorithm 1 Roundabout Maneuver System Planner

Initialization: while the ego car approaches the roundabout
 The ego car decides on the mission
repeat
 Select appropriate lane before entering the roundabout;
 Yield to pedestrians in the crosswalk;
 Drive on the global planner path;
 Confirm the roundabout geometry parameters;
 Select waypoints based on the entry radius and entrance angle phi
 Start B-spine generator and tracking controller
until Update state function and travels through the roundabout successfully
Output: The vehicle completes the mission and passes through the roundabout

parameters of single-lane roundabouts in different countries. The waypoints and road constraints are defined according to the entry and exit allowed by each country’s standards and the roundabout’s structural characteristics.

TABLE 1. Geometry parameters of single-lane roundabout.

Geometry parameters	Standard area	Single-lane roundabout
Entry angle	UK	20°–40°
	Swiss	45°–90°
	German	–
	US	20°–60°
Entry radius	UK	≤ 100 m
	Swiss	–
	German	≥ 14 m ≤ 18 m
	US	≥ 15 m ≤ 30 m
Exit radius	UK	–
	Swiss	–
	German	≥ 16 m ≤ 18 m ≥ 15 m, with values of 30 to 60 m being more common
	US	≥ 28 m ≤ 36 m
Circle Diameter	Swiss	≥ 27 m ≤ 40 m
	German	≥ 30 m ≤ 50 m
	US	≥ 27 m ≤ 54 m

Considering the safety and comfort of vehicle driving, the lateral acceleration constraint of the vehicle is as follows

$$-1m/s^2 < \dot{v}_{la} < 1m/s^2 \tag{8}$$

To protect vehicles from moving off the road, set the value of the feasible domain boundary in the road coordinate system to be a half-car width away from the edge of the road

$$\left(S_{L\min} + \frac{W_c}{2} \right) \leq S \leq \left(S_{L\max} - \frac{W_c}{2} \right) \tag{9}$$

As shown in Figure 2, $S_{L\max}/S_{L\min}$ are the limit position offsets of the right/left road boundary, respectively, and W_c represents the vehicle width.

IV. SYSTEM PLANNER GENERATION
A. MANEUVER PLANNING DEFINITION

There are two main mathematical methods used in trajectory planning. One is the polynomial interpolation method, including Lagrangian interpolation and Newton’s interpolation; the other is the spline curve interpolation method.

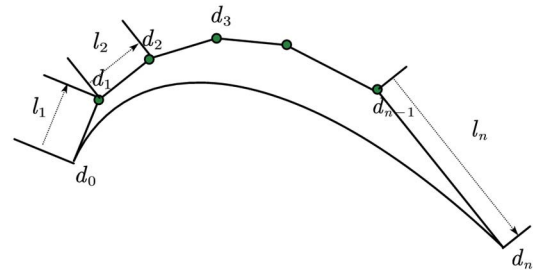


FIGURE 3. Cubic B spline curve piecewise segment connection points correspond to control polygons.

Spline interpolation was originally used for function fitting. In contrast to the cubic polynomial interpolation method, it is more realistic that the curve is fitted by the spline interpolation method in the roundabout. The useful properties of B-spline based interpolation algorithm can be listed as follows, which also present the B-spline curve advantages:

- Continuity and smoothness of the spline curve is assured at the connection point.
- The first and second-order derivatives of the cubic spline are continuous.
- A single knot does not affect the whole interpolation line due to the local supportive property. It is much more convenient for a vehicle to modify the path point datasets and control points during driving.

Control points determine the weight of each part function in the spline shaping. The relationship between control points and knot vectors for each spline segment is represented as (3).

We were given a set of data points $P = p_0, \dots, p_n \in R_d$. The first and last data points p_0 and p_n are used as the first and last points of the cubic B-spline interpolation curve. The internal data points p_1, p_2, \dots, p_{n-1} can be seen as the piecewise segment connection points of the cubic B-spline interpolation curves in turn, then the curves are in n segments. This section needs to select the appropriate parameterization method to back-calculate the control points according to the distribution of data points.

The knot vectors of the cubic B-spline segment can be obtained respectively. The B-spline path is a piecewise vector function, and due to the local support property of the B-spline, a cubic B-spline path is affected by only four control points. Assume that segment connection points of the spline curve correspond to the control polygon’s remaining control points, except for each segment’s position. Expanding and normalizing them, the knots vector formulation is

$$U = \left[0, 0, 0, 0, \frac{l_1 + l_2}{L}, \frac{l_1 + l_2 + l_3}{L}, \dots, \frac{l_1 + l_2 + \dots + l_{n-2}}{L}, 1, 1, 1, 1 \right] \tag{10}$$

In the roundabout scenario, the data points are collected mainly from the middle point of the yield line and the midpoint of each of the circulatory roadway’s eighths.

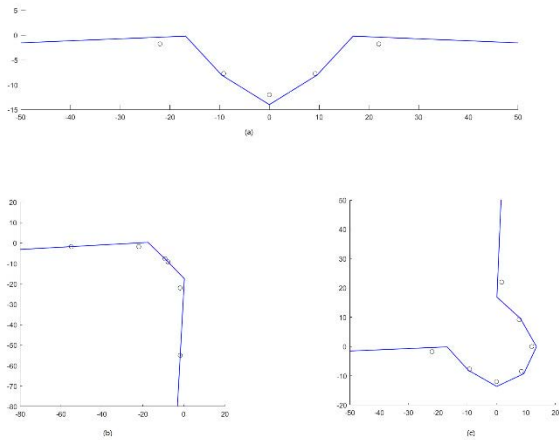


FIGURE 4. The same roundabout entrance to three different exits selected data points (circle) and their control polygons (blue line).

As Figure 4 shows, the black circles are the data points collected from the roundabout model. Each data point is also the connection point of adjacent sections. In this way, the B-spline curve can be calculated piece by piece in the scenario. Select different data points selection will change the curve shape. As Figure 5 illustrates, the last control point has good performance on parameterization method interpolation. When the number of data points changes, the control points affect the spline curve shape, but three curves constructed by different knot vectors pass through the data points collected from the roundabout model.

We align the first and last points of the curve with the first and last data points, respectively. The first and last control points of a curve with a knot vector can be described as

$$T = \left(\underbrace{t_0, t_1, \dots, t_{k-1}}_{k \text{ equalknots}}, \underbrace{t_k, t_{k+1}, \dots, t_{n-1}}_{n-k+1 \text{ internalknots}}, \underbrace{t_n, t_{n+1}, \dots, t_{n+k}}_{k \text{ equalknots}} \right) \quad (11)$$

B. PATH CONTROL POINTS SOLVING BASED ON KNOTS VECTOR

In this study, the cubic B-spline interpolation algorithm is used to generate the path and the control points $b_i, i = 1, 2, \dots, n - 3$. The initial control point can be expressed by $P_i(u_{i+3})$

$$= B_i(u_{i+3}) B_{i+1}(u_{i+3}) B_{i+2}(u_{i+3}) B_{i+3}(u_{i+3}) \begin{bmatrix} V_i \\ V_{i+1} \\ V_{i+2} \\ V_{i+3} \end{bmatrix} \quad (12)$$

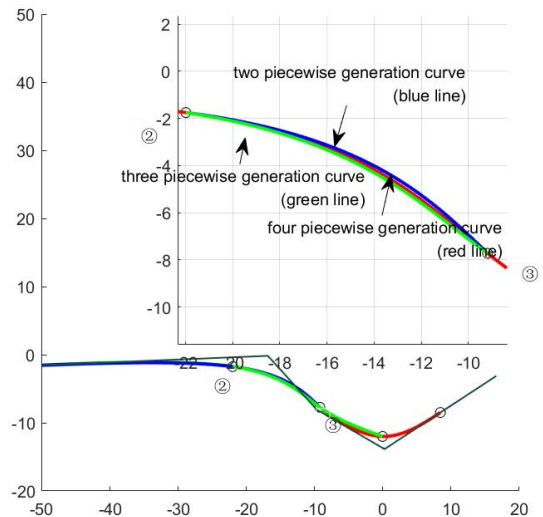


FIGURE 5. Different pieces curves generation.

(u_{i+3}) represents the parameter value of the initial point, $i \in [0, m - 4]$. From (12), $m - 3$ piecewise section, initial knots can be obtained. The control point calculation matrix can be expressed as follows

$$\begin{cases} P_0 = V_0 \\ P_i(u_{i+3}) = \\ B_i(u_{i+3}) B_{i+1}(u_{i+3}) B_{i+2}(u_{i+3}) B_{i+3}(u_{i+3}) \\ P_{n-1} = V_{m-1} \end{cases} \begin{bmatrix} V_i \\ V_{i+1} \\ V_{i+2} \\ V_{i+3} \end{bmatrix} \quad (13)$$

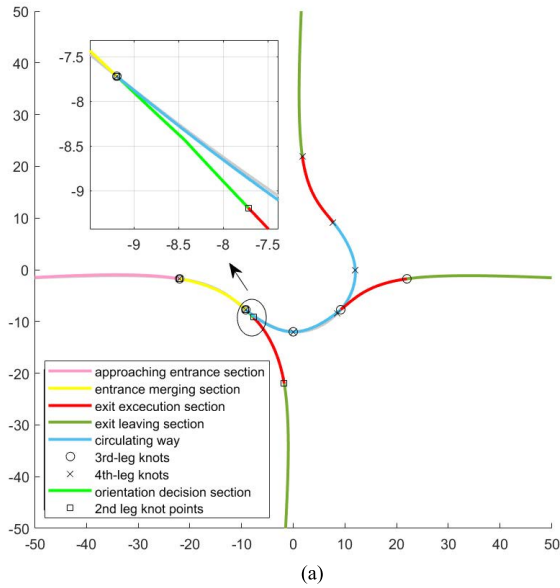
The equation has m unknowns, and two additional end-point conditions are needed to solve the equation. The linear equation transfer to the matrix is as follows. Equation (14), as shown at the bottom of the previous page.

C. B-spline BASED PATH GENERATION

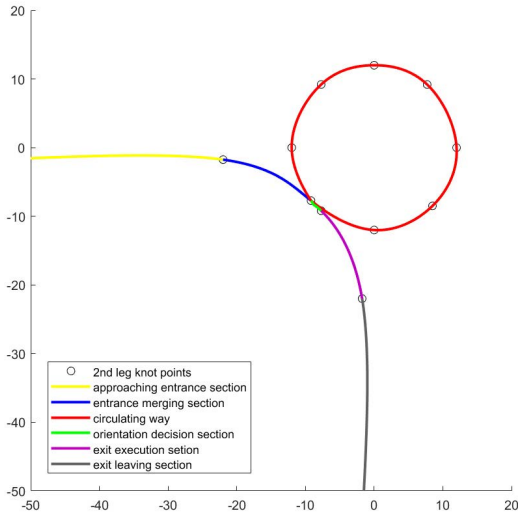
The selection of the actual data points depends on the change of the preset path driving decision, and the fixing of the selection points completes the section of data points for the whole driving route.

As shown in Figure 6(a), (b), (c), the whole route map of five kinds of roundabout exit cases are shown, respectively.

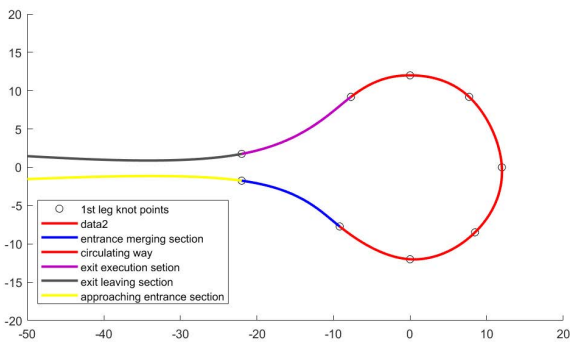
$$\begin{bmatrix} B_{1,3}(u_3) & B_{2,3}(u_3) & & B_{0,3}(u_3) \\ B_{1,3}(u_4) & B_{2,3}(u_3) & B_{3,3}(u_3) & \\ \dots & & & \\ \dots & B_{n-4,3}(u_3) & B_{n-3,3}(u_3) & B_{n-2,3}(u_3) \\ B_{n-1,3}(u_3) & & B_{n-3,3}(u_3) & B_{n-2,3}(u_3) \end{bmatrix} \begin{bmatrix} V_1 \\ V_2 \\ \dots \\ V_{n-3} \\ V_{n-4} \end{bmatrix} = \begin{bmatrix} q_0 \\ q_1 \\ \dots \\ q_{n-4} \\ q_{n-3} \end{bmatrix} \quad (14)$$



(a)



(b)



(c)

FIGURE 6. (a) The paths connect the entrance, circulating roadway, and different angle exits smoothly. (b) Piecewise B-spline path planning through the circulating way to a new exit, this case is an example for driving miss out the second leg, and driving back through the circulatory roadway. (c) Path generates a U-turn entrance-exit maneuver.

The maneuver to the second exit leg is symmetric. We defined the second data point as the starting point of the merging zone, the third and fourth points making the decision difference from other exit reference paths, as shown in the Figure 6(a) zoomed picture. After the fourth data point, the vehicle makes the execution to join the first exit leg, and a yellow path means the vehicle has already traversed the roundabout. The path generation to the third leg and fourth leg has a common period in circulating, which means the knots vectors setting on the circulating way should be the same.

The common denominator between the U-turn and driving miss-out to the first leg cases path generation is waypoints on the circulatory roadway. Since the two cases, as shown in Figures 6(b) and (c), are mainly composed of a roundabout inner circle and a merging zone path. The knot vectors should be set according to their driving decision orientation; the merging points of the entrance and exit section are the middle point of the circulating circle's yield line and the octant point. The paths are generated piece by piece after solving the control point calculation.

D. TRACKING CONTROL LAWS

The Stanley controller is based on the concept of cross-track error. Calculating the cross-track error: e , the orthogonal length make from the middle point of the front axle on path point (s_x, s_y) , set a nonlinear function and achieve convergence of the cross-track error exponent to 0. $\delta(t)$ represents the control variables, controlling the steering wheel angle that can be obtained intuitively from the relative geometry of the vehicle attitude and the given path, which include the cross-track error e and the heading deviation θ_e in (15)

$$\delta(t) = \delta_e(t) + \delta_{\theta_e}(t) \tag{15}$$

The lateral tracking error represents the stabilization of the vehicle. The prospective trajectory of the ego vehicle make out the distance $d(t)$, the tangent of the nearest point on the given path from the front wheels. The following function illustrates the relationship clearly,

$$\delta_e(t) = \arctan \frac{e(t)}{d(t)} = \arctan \frac{ke(t)}{v(t)} \tag{16}$$

where $d(t)$ is connected with the vehicle speed and expressed in terms of the vehicle speed $v(t)$ involving the gain parameter k . The arctan function shows a front-wheel deviation that faces the desired path, and the vehicle speed limits the convergence $v(t)$. The steering control law can be shown as,

$$\delta_e(t) = \theta_e(t) + \arctan \frac{ke(t)}{v(t)} \tag{17}$$

and the derivative of the cross-track error is

$$\dot{e}(t) = v(t)\sin(\theta(t) - \delta(t)) \tag{18}$$

In this work, the circle diameter is set to be 32 m. Each run sets the initial point and endpoint and chooses different knot vectors to reach global planning. In this section, recurve path cases are presented as well. Case studies (c), (d), and

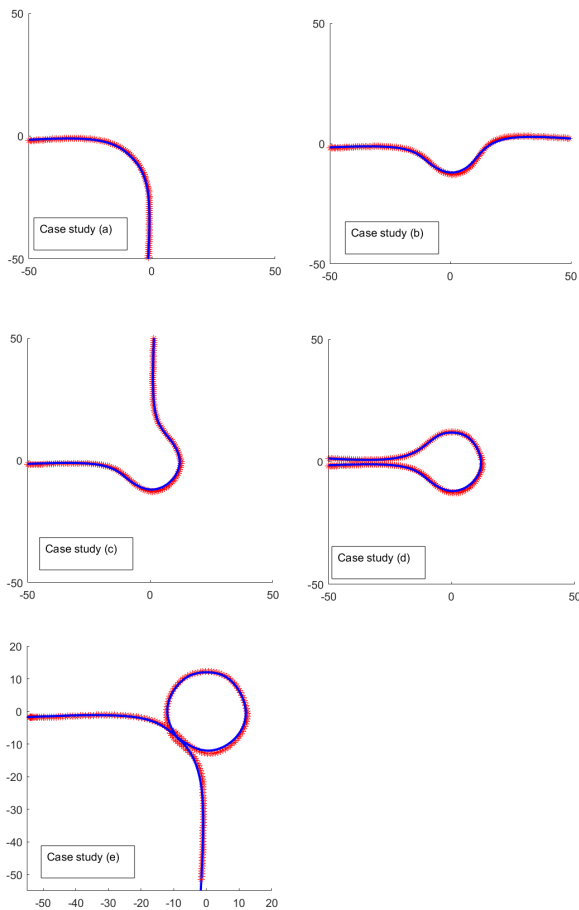


FIGURE 7. The implementation of five study cases of the vehicle at the roundabout. The blue line is path planning results; the red dots line is the tracking route of each study case.

(e) represent special cases in driving scenarios, as the planner needs to switch into the back points as the vehicle makes the decision to travel to different legs.

V. EXPERIMENTAL RESULTS AND DISCUSSION

In the results presented in this section, the piecewise B-spline method generates roundabout entrance, circulating road, and different exit direction paths and connects them smoothly; the Stanley tracking controller verifies the continuity and comfort of paths. Sections 5.1 and 5.2 build the model based on two circle diameter limits.

As shown in Figure 8, the roundabout test framework illustrates the main procedure of the whole test. For different driving directions, segmentation of the route and their waypoints selection will be introduced more specifically in Table2. The algorithm and simulation were implemented in MATLAB 2021b. The commands settings are as follows: the wheelbase of the vehicle is 2.6m, the simulation step is 0.01s, the system planner and solution are using MATLAB Function to build, and the path data are stored and loaded via mat. file in MATLAB.

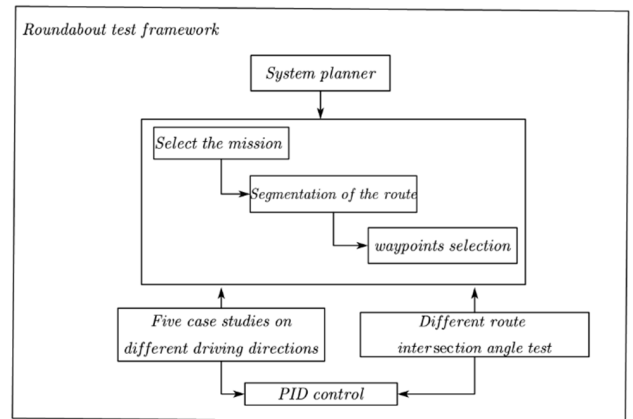


FIGURE 8. Roundabout test framework.

A. FIVE CASE STUDIES ON DIFFERENT DRIVING DIRECTIONS

As shown in Figure 7, the geometric result has been illustrated by the path planning phase. In this section, we mainly discuss the path tracking results of the five case studies.

Figure 9(a) to Figure 9(e) correspond to the five global planning study cases; all the cases were tested on the yaw, the velocity, and the cross track error parameters.

Figure 9(a) shows the maneuver that goes directly to the second exit, and the cross-track error was changing a bit rapidly at the curve generation part. In this study case, the gain parameter was set to $k = 0.01$. Figure 9(b) is the vehicle that travels through the third exit, with the same parameter settings as the previous study case. We simulated the cross-track error and yaw value. It can be noted that the cross-track error changes more significantly when the path curvature is more extensive.

In Figures 9(c), (d), and (e), the paths all travel through the majority of the circulating way, which means the last index of the route cannot be the length of the reference path x -axis vector. The paths all have different degrees of recurve, and the cross-track error changes based on their path recurve character. It is clear that in Figures 9(c) and (d), the paths are recurved once, Figure 9(e) has a recurved period twice.

The longitudinal controller was set as a PI controller to manage the speed profile and choose the target speed of 30 km/h. From the figures above, the velocity is maintained in a stable section.

B. MANEUVER GENERATION BASED ON INTERSECTION ANGLES

In this section, the system planner test in thirteen groups. The Table 2 demonstrates each group’s specific test parameters, i.e., the roundabout outer radius, entry radius, exit radius, and intersection angle of roundabout legs. Waypoints selection follows the rule in the system planner, segment the route into

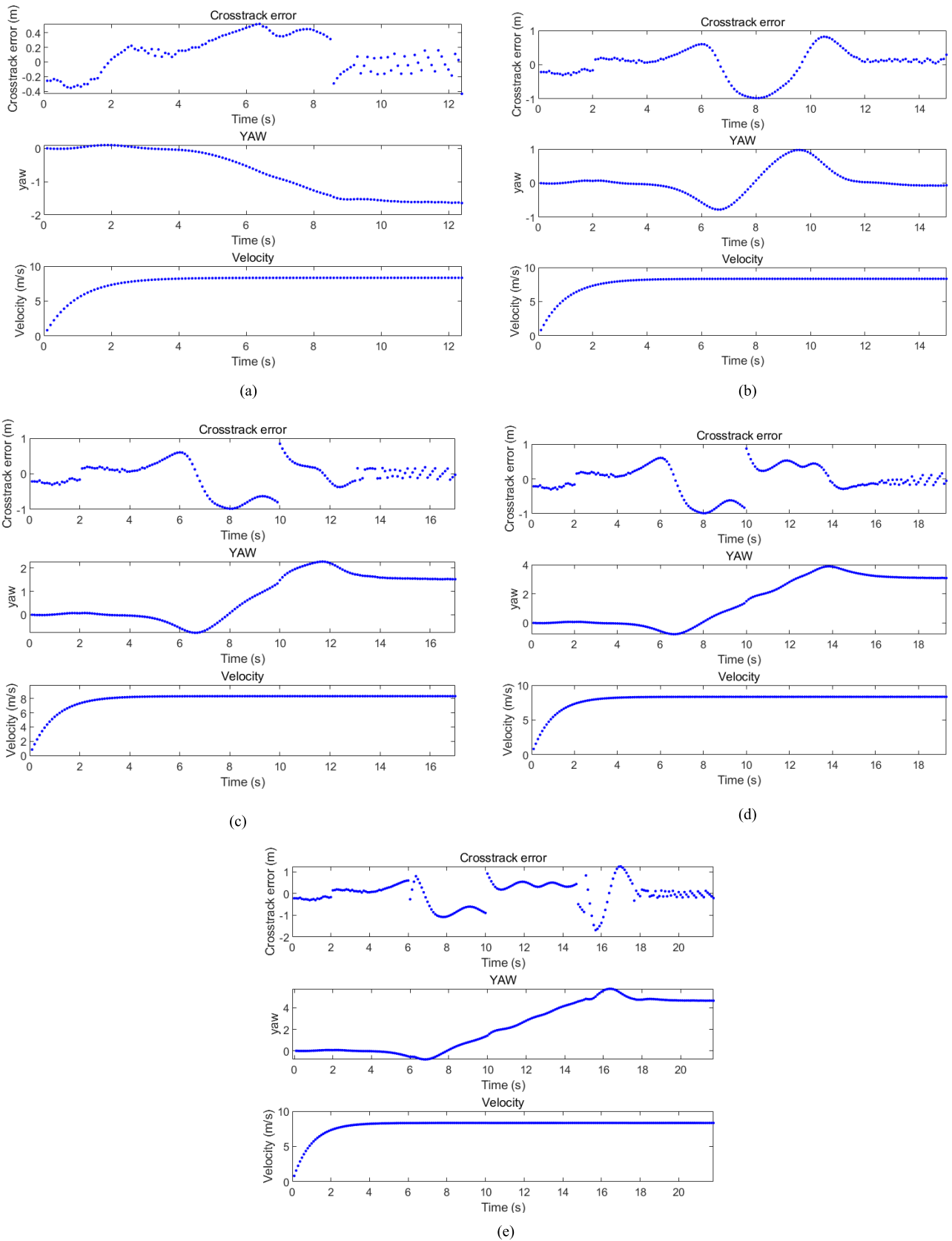


FIGURE 9. (a) The second leg case of maneuver planner at the roundabout. (b) The third leg case of maneuver planner at the roundabout. (c) The fourth leg case of maneuver planner at the roundabout. (d) The U-turn leg case of maneuver planner at the roundabout. (e) The missing-out leg case of maneuver planner at the roundabout.

TABLE 2. Path elements data in intersection angles ranged from 60 to 120°, with a 5° increment.

GROUP	OUTER RADIUS (M)	ENTRY FILLET RADIUS (%)	ENTRY FILLET RADIUS (%)	INTERSECTION ANGLE (°)	DETERMINED WAYPOINTS COORDINATES		
					APPROACHING ZONE	INNER CIRCLE ZONE	EXIT ZONE
1	25	60	65	60	-68.68,-1.57,0; -38.68,-1.86,0;	-24.73,-6.06,0; -19.61,-12.71,0; -17,-22,0;	-21.13,-33.70,0; -35.97,-59.77,0
2	25	60	65	65	-68.68,-1.57,0; -38.42,-1.86,0;	-24.26,-6.27,0; -19.36,-11.82,0; -15.08,-24.10,0; -16.67,-32.50,0;	-18.11,-35.53,0; -30.51,-62.74,0
3	25	60	65	70	-68.68,-1.57,0; -37.68,-1.86,0;	-24.51,-6.63,0; -19.57,-11.07,0; -14.34,-18.83,0;	-14.01,-33.95,0; -24.57,-65.27,0
4	25	60	65	75	-68.68,-1.57,0; -38.68,-1.86,0;	-24.63,-5.98,0; -18.34,-12.53,0; -13.53,-19.37,0;	-10.18,-32.84,0; -18.27,-65.05,0
5	25	60	65	80	-68.68,-1.92,0; -38.68,-1.86,0;	-24.79,-5.71,0; -18.34,-12.53,0; -13.53,-19.37,0;	-8.19,-38.41,0; -13.68,-67.42,0
6	25	60	65	85	-68.68,-1.92,0; -38.68,-1.86,0;	25.20,-5.35,0; -18.26,-12.32,0; -13.05,-17.48,0; -8.33,-21.99,0;	-4.91,-35.09,0; -7.03,-67.75,0
7	25	60	65	90	-68.68,-1.98,0; -38.17,-1.93,0;	-24.84,-5.64,0; -19.20,-10.75,0; -13.52,-17.10,0; -7.65,-22.80,0;	-1.98,-36.37,0; -1.98,-69.24,0
8	25	60	65	95	-68.68,-1.98,0; -38.17,-1.93,0;	-24.84,-5.64,0; -16.75,-13.78,0; -9.47,-20.13,0; -2.56,-26.73,0;	1.55,36.56,0; 5.27,-69.21,0
9	25	60	65	100	-68.68,-1.98,0; -38.17,-1.93,0;	-26.13,-5.41,0; -18.88,-11.37,0; -6.87,-20.85,0;	4.91,-36.77,0; 11.90,-69.66,0
10	25	60	65	105	-68.68,-1.98,0; -38.17,-1.93,0;	-26.13,-5.41,0; -18.88,-11.37,0; -5.09,-21.30,0;	7.73,-35.84,0; 17.42,-68.04,0
11	25	60	65	110	-68.68,-1.98,0; -38.17,-1.93,0;	-25.35,-5.54,0; -17.75,-12.73,0; -4.69,-21.65,0;	10.81,-34.50,0; 23.30,-66.15,0
12	25	60	65	115	-68.68,-1.98,0; -38.17,-1.93,0;	-24.79,-5.71,0; -18.34,-12.73,0; -6.20,-20.93,0;	14.39,-36.03,0; 27.35,-63.78,0
13	25	60	65	120	-68.68,-1.98,0; -38.17,-1.93,0;	-24.50,-6.89,0; -18.55,-13.15,0; -2.29,-21.54,0;	16.74,33.21,0; 32.75,-61.36,0

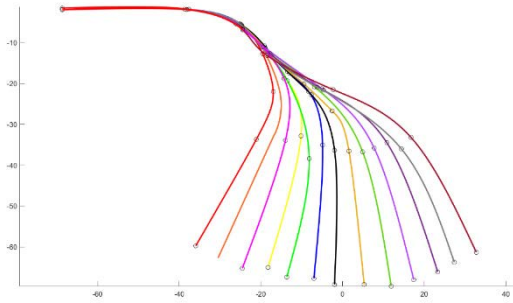


FIGURE 10. Path illustration in intersection angles ranged from 60 to 120°, with a 5° increment.

the roundabout approaching zone, inner circle zone, and exit zone.

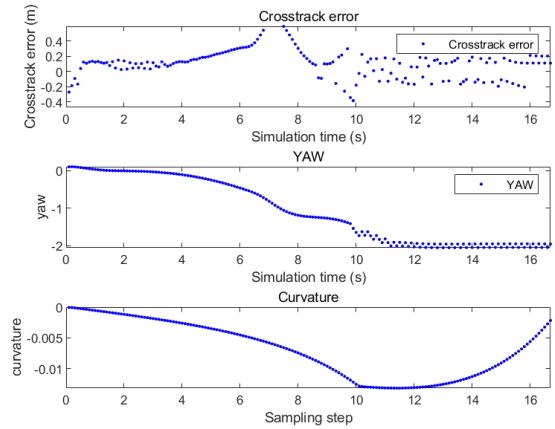
As shown in Figure 10, the path was generated successfully on intersection angles ranging from 60° to 120° by determined waypoints. The waypoints in Table 2 determine the structure of the path polygon, satisfy the road constraints, and the uniform B-spline method takes advantage of path smoothing. The circle diameter is set to 50 m. The entry fillet radius is set as 60 percentage of the outer radius. The exit fillet radius sets larger than the entry radius because of the roundabout design standard [36]. As the intersection angle increases, the path elements via the circulatory roadway generate more waypoints.

Figures 11 (a), (b), (c) were the chosen to be the validation tests from group intersection angle 60° to 120°. The vehicle heading changes significantly when intersection angle becomes larger. The curvature calculations are based on the real time x and y values, and the cross track error is distributed dispersedly when curvature data approach back to 0.

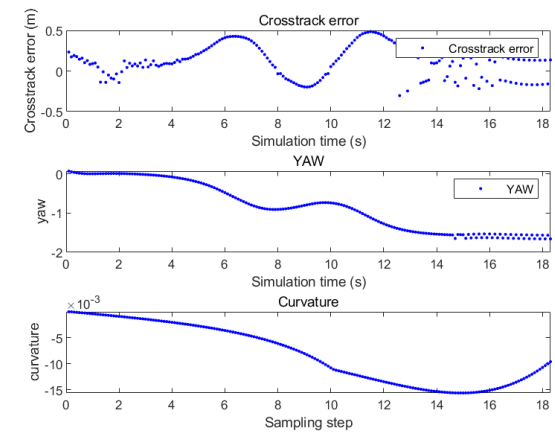
VI. CONCLUSION

Applying the basic traffic rules and normal vehicle behaviors at roundabouts, this paper presents autonomous vehicle path planning methods taking different exits, and combines the geometric design elements of the road with the maneuverability of the vehicle path design. The defined waypoints take an important role on path structure and driving direction. In the case of a right turn, the vehicle has the smallest path radius and is expected to develop a lower speed than the other possible travel directions. In the case of a straight-through traffic circle or left turn, the path radius and vehicle speed information are proven to be greatest. One of the limitations of this study is that in the modeled case, the longitudinal slope of the intersection leg is approximately horizontal.

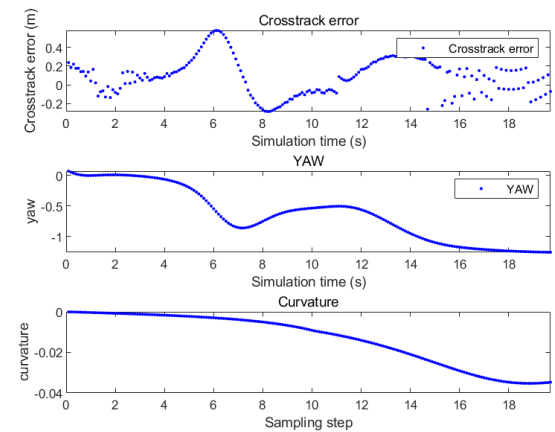
After data set building, the piecewise uniform B-spline interpolation method was employed to schedule the knot vectors path. The planner meets the path smooth requirement, especially in the continuous large curvature road condition. Our work is based on the special geometric structure of the roundabout, calculates the control points from knot vectors, and solves the planner with the piecewise uniform



(a)



(b)



(c)

FIGURE 11. (a) Path elements data on intersection angle 70°. (b) Path elements data on intersection angle 90°. (c) Path elements data on intersection angle 110°.

B-spline basis function. Simulation results illustrate that the presented method could generate a trajectory that meets the required constraints and meets the roundabout recurve path condition. Moreover, the speed profile satisfies vehicle stability requirements, road constraints, and necessary comfort conditions.

REFERENCES

- [1] M. Zoldy, M. S. Csete, P. P. Kolozsi, P. Bordas, and A. Torok, "Cognitive sustainability," *Cognit. Sustainability*, vol. 1, no. 1, Mar. 2022, doi: [10.55343/cogsust.7](https://doi.org/10.55343/cogsust.7).
- [2] T. Maekawa, T. Noda, S. Tamura, T. Ozaki, and K.-I. Machida, "Curvature continuous path generation for autonomous vehicle using b-spline curves," *Comput.-Aided Des.*, vol. 42, no. 4, pp. 350–359, Apr. 2010.
- [3] T. Ort, L. Paull, and D. Rus, "Autonomous vehicle navigation in rural environments without detailed prior maps," in *Proc. IEEE Int. Conf. Robot. Autom. (ICRA)*, May 2018, pp. 2040–2047, doi: [10.1109/ICRA.2018.8460519](https://doi.org/10.1109/ICRA.2018.8460519).
- [4] K. Karur, N. Sharma, C. Dharmatti, and J. E. Siegel, "A survey of path planning algorithms for mobile robots," *Vehicles*, vol. 3, no. 3, pp. 448–468, 2021, doi: [10.3390/vehicles3030027](https://doi.org/10.3390/vehicles3030027).
- [5] H. Kano and H. Fujioka, "B-spline trajectory planning with curvature constraint," in *Proc. Annu. Amer. Control Conf. (ACC)*, Jun. 2018, pp. 1963–1968.
- [6] R. Goldenthal and M. Bercovier, "Spline curve approximation and design by optimal control over the knots," *Computing*, vol. 72, pp. 53–64, Apr. 2004.
- [7] D. González, J. Pérez, and V. Milanés, "Parametric-based path generation for automated vehicles at roundabouts," *Expert Syst. Appl.*, vol. 71, pp. 332–341, Apr. 2017, doi: [10.1016/j.eswa.2016.11.023](https://doi.org/10.1016/j.eswa.2016.11.023).
- [8] L. Chen, D. Qin, X. Xu, Y. Cai, and J. Xie, "A path and velocity planning method for lane changing collision avoidance of intelligent vehicle based on cubic 3-D Bezier curve," *Adv. Eng. Softw.*, vol. 132, pp. 65–73, Jun. 2019.
- [9] H. Cao and M. Zöldy, "An investigation of autonomous vehicle roundabout situation," *Periodica Polytechnica Transp. Eng.*, vol. 48, no. 3, pp. 236–241, 2020, doi: [10.3311/PPTr.13762](https://doi.org/10.3311/PPTr.13762).
- [10] J. Moreau, P. Melchior, S. Victor, M. Moze, F. Aioun, and F. Guillemard, "Reactive path planning for autonomous vehicle using Bézier curve optimization," in *Proc. IEEE Intell. Vehicles Symp. (IV)*, Jun. 2019, pp. 1048–1053, doi: [10.1109/ivs.2019.8813904](https://doi.org/10.1109/ivs.2019.8813904).
- [11] D. González, J. Pérez, V. Milanés, and F. Nashashibi, "A review of motion planning techniques for automated vehicles," *IEEE Trans. Intell. Transp. Syst.*, vol. 17, no. 4, pp. 1135–1145, Nov. 2016, doi: [10.1109/tits.2015.2498841](https://doi.org/10.1109/tits.2015.2498841).
- [12] M. Mischinger, M. Rudigier, P. Wimmer, and A. Kerschbaumer, "Towards comfort-optimal trajectory planning and control," *Vehicle Syst. Dyn.*, vol. 57, pp. 1–18, Dec. 2018, doi: [10.1080/00423114.2018.1551553](https://doi.org/10.1080/00423114.2018.1551553).
- [13] D. Devaurs, T. Siméon, and J. Cortés, "Parallelizing RRT on large-scale distributed-memory architectures," *IEEE Trans. Robot.*, vol. 29, no. 2, pp. 571–579, Apr. 2013, doi: [10.1109/TRO.2013.2239571](https://doi.org/10.1109/TRO.2013.2239571).
- [14] H. Prautzsch, W. Boehm, and M. Paluszny, "Bézier and B-spline techniques," Tech. Rep., 2002, doi: [10.1007/978-3-662-04919-8](https://doi.org/10.1007/978-3-662-04919-8).
- [15] L. Han, H. Yashiro, H. Tehrani, H. Do, and S. Mita, "Bézier curve based path planning for autonomous vehicle in urban environment," in *Proc. IEEE Intell. Vehicles Symp.*, Jun. 2010, pp. 1036–1042, doi: [10.1109/IVS.2010.5548085](https://doi.org/10.1109/IVS.2010.5548085).
- [16] P. Koch and K. Wang, "Introduction of B-splines to trajectory planning for robot manipulators," *Model., Identificat. Control*, vol. 9, no. 2, pp. 69–80, 1988, doi: [10.4173/mic.1988.2.2](https://doi.org/10.4173/mic.1988.2.2).
- [17] L. H. Pérez, M. C. M. Aguilar, N. M. Sánchez, and A. F. Montesinos, "Path planning based on parametric curves," in *Advanced Path Planning for Mobile Entities*. London, U.K.: IntechOpen, 2017, doi: [10.5772/intechopen.72574](https://doi.org/10.5772/intechopen.72574).
- [18] M. Gloderer and A. Hertle, "Spline-based trajectory optimization for autonomous vehicles with Ackerman drive," Tech. Rep., 2010.
- [19] J. Connors and G. Elkaim, "Manipulating b-spline based paths for obstacle avoidance in autonomous ground vehicles," in *Proc. ION Nat. Tech. Meeting*, 2007, pp. 1081–1088.
- [20] T. Berglund, A. Brodnik, H. Jonsson, M. Staffanson, and I. Söderkvist, "Planning smooth and obstacle-avoiding B-spline paths for autonomous mining vehicles," *IEEE Trans. Autom. Sci. Eng.*, vol. 7, no. 1, pp. 167–172, Jan. 2010.
- [21] F. Ghilardelli, G. Lini, and A. Piazzzi, "Path generation using η^4 splines for a truck and trailer vehicle," *IEEE Trans. Automat. Sci. Eng.*, vol. 11, no. 1, pp. 187–203, Jan. 2014.
- [22] T. Mercy, R. Van Parys, and G. Pipeleers, "Spline-based motion planning for autonomous guided vehicles in a dynamic environment," *IEEE Trans. Control. Syst. Technol.*, vol. 26, no. 6, pp. 2182–2189, Nov. 2018.
- [23] F. Ahmed and K. Deb, "Multi-objective path planning using spline representation," in *Proc. IEEE Int. Conf. Robot. Biomimetics*, Dec. 2011, pp. 1047–1052.
- [24] C. de Boor, *A Practical Guide to Splines*. Cham, Switzerland: Springer, 1978.
- [25] D. Ji, J. Liu, H. Zhao, and Y. Wang, "Path following of autonomous vehicle in 2D space using multivariable sliding mode control," *J. Robot.*, vol. 2014, pp. 1–6, Jan. 2014, doi: [10.1155/2014/217875](https://doi.org/10.1155/2014/217875).
- [26] M. A. Daoud, M. W. Mehrez, D. Rayside, and W. W. Melek, "Simultaneous feasible local planning and path-following control for autonomous driving," *IEEE Trans. Intell. Transp. Syst.*, early access, Feb. 23, 2022, doi: [10.1109/TITS.2022.3149986](https://doi.org/10.1109/TITS.2022.3149986).
- [27] R. Liu, M. Wei, N. Sang, and J. Wei, "Research on curved path tracking control for four-wheel steering vehicle considering road adhesion coefficient," *Math. Problems Eng.*, vol. 2020, pp. 1–18, Jan. 2020, doi: [10.1155/2020/3108589](https://doi.org/10.1155/2020/3108589).
- [28] X. Li, Z. Sun, D. Cao, D. Liu, and H. He, "Development of a new integrated local trajectory planning and tracking control framework for autonomous ground vehicles," *Mech. Syst. Signal Process.*, vol. 87, pp. 118–137, Mar. 2017, doi: [10.1016/j.ymsp.2015.10.021](https://doi.org/10.1016/j.ymsp.2015.10.021).
- [29] C. Huang, B. Li, and M. Kishida, "Model predictive approach to integrated path planning and tracking for autonomous vehicles," in *Proc. IEEE Intell. Transp. Syst. Conf. (ITSC)*, Oct. 2019, pp. 1448–1453, doi: [10.1109/itsc.2019.8916898](https://doi.org/10.1109/itsc.2019.8916898).
- [30] H. Cao and M. Zoldy, "MPC tracking controller parameters impacts in roundabouts," *Mathematics*, vol. 9, no. 12, p. 1394, 2021, doi: [10.3390/math9121394](https://doi.org/10.3390/math9121394).
- [31] C. Ko, S. Han, M. Choi, and K.-S. Kim, "Integrated path planning and tracking control of autonomous vehicle for collision avoidance based on model predictive control and potential field," in *Proc. 20th Int. Conf. Control, Autom. Syst. (ICCAS)*, Oct. 2020, pp. 956–961.
- [32] K. D. Ellenrieder, S. Licht, R. Belotti and H. Henninger, "Shared human-robot path following control of an unmanned ground vehicle," *Mechatronics*, vol. 83, May 2022, Art. no. 102750, doi: [10.1016/j.mechatronics.2022.102750](https://doi.org/10.1016/j.mechatronics.2022.102750).
- [33] J. Ahn, S. Shin, and M. Kim, "Accurate path tracking by adjusting look-ahead point in pure pursuit method," *Int. J. Autom. Technol.*, vol. 22, pp. 119–129, Feb. 2021, doi: [10.1007/s12239-021-0013-7](https://doi.org/10.1007/s12239-021-0013-7).
- [34] N. H. Amer, H. Zamzuri, and K. Hudha, "Path tracking controller of an autonomous armoured vehicle using modified Stanley controller optimized with particle swarm optimization," *J. Braz. Soc. Mech. Sci. Eng.*, vol. 40, p. 104, Jan. 2018, doi: [10.1007/s40430-017-0945-z](https://doi.org/10.1007/s40430-017-0945-z).
- [35] S. Dominguez, A. Ali, G. Garcia, and P. Martinet, "Comparison of lateral controllers for autonomous vehicle: Experimental results," in *Proc. IEEE 19th Int. Conf. Intell. Transp. Syst. (ITSC)*, Nov. 2016, pp. 1418–1423.
- [36] B. W. Robinson, *Roundabouts: An Informational Guide*, document FHWA-RD-00-067, Federal Highway Administration, 2000.
- [37] L. H. Pérez, M. C. M. Aguilar, N. M. Sánchez, and A. F. Montesinos, "Path planning based on parametric curves," in *Advanced Path Planning for Mobile Entities*. London, U.K.: IntechOpen, 2017, doi: [10.5772/intechopen.72574](https://doi.org/10.5772/intechopen.72574).
- [38] H. Kano and H. Fujioka, "B-spline trajectory planning with curvature constraint," in *Proc. Annu. Amer. Control Conf. (ACC)*, Jun. 2018, pp. 1963–1968.
- [39] M. Elbanhawi, M. Simic, and R. N. Jazar, "Solutions for path planning using spline parameterization," in *Nonlinear Approaches in Engineering Applications*, L. Dai and R. Jazar, Eds. Cham, Switzerland: Springer, 2018.
- [40] N. Evestedt, E. Ward, J. Folkesson, and D. Axehill, "Interaction aware trajectory planning for merge scenarios in congested traffic situations," in *Proc. IEEE 19th Int. Conf. Intell. Transp. Syst. (ITSC)*, Nov. 2016, pp. 465–472.
- [41] Y. J. Kanayama and B. I. Hartman, "Smooth local-path planning for autonomous vehicles," *Int. J. Robot. Res.*, vol. 16, no. 3, p. 263, 1997.
- [42] L. Chen, D. Qin, X. Xu, Y. Cai, and J. Xie, "A path and velocity planning method for lane changing collision avoidance of intelligent vehicle based on cubic 3-D Bezier curve," *Adv. Eng. Softw.*, vol. 132, pp. 65–73, Jun. 2019.
- [43] H.-C. Chang and J.-S. Liu, "High-quality path planning for autonomous mobile robots with η_3 -splines and parallel genetic algorithms," in *Proc. IEEE Int. Conf. Robot. Biomimetics*, Feb. 2009, pp. 1671–1677.
- [44] H. P. Seidel, "Computing B-spline control points," in *Theory and Practice of Geometric Modeling*, W. Straßer and H. P. Seidel, Eds. Berlin, Germany: Springer, 1989.

- [45] X. D. Chen, W. Y. Ma, and J.-C. Paul, "Cubic B-spline curve approximation by curve unclamping," *Comput.-Aided Des.*, vol. 42, no. 6, pp. 523–534, 2010, doi:[10.1016/j.cad.2010.01.008](https://doi.org/10.1016/j.cad.2010.01.008).



HANG CAO received the master's degree in vehicle engineering from the Budapest University of Technology and Economics, in 2019, where she is currently pursuing the Ph.D. degree with the Department of Automotive Technologies. Her current research interests include driving maneuver, decision making, and uncertainties.



MATE ZOLDY received the M.Sc. and Ph.D. degrees in vehicle engineering and the M.Sc. degree in economics.

He is the Head of the Innovative Vehicle Technologies Research Laboratory with the Department of Automotive Technologies, Budapest University of Technology and Economics. He has more than ten years of experience from oil and gas industry at MOL Group and another five years in automotive industry (Ford and AVL). He initiated and lead developments, as XXL Diesel—a special product for niche markets. His main research interests include cognitive sustainability and cognitive mobility with special focus on vehicle and fuel technologies. He was a recipient of the Best paper Award from the IEEE 12th Coginfocom Conference, in 2021.

• • •